Long-Range Distance Constraints in Platinated Nucleotides: Structure Determination of the 5′ Orientational Isomer of *cis*-[Pt(NH$_3$)(4-aminoTEMPO){d(GpG)}]$^+$ from Combined Paramagnetic and Diamagnetic NMR Constraints with Molecular Modeling

Stephen U. Dunham and Stephen J. Lippard*

Contribution from the Department of Chemistry, Massachusetts Institute of Technology, Cambridge, Massachusetts 02139

Received March 14, 1995[⊗]

Abstract: The compound *cis*-[Pt(NH$_3$)(4-aminoTEMPO)Cl] (**7**) is a paramagnetic analogue of the anticancer drug cisplatin and of *cis*-[Pt(NH$_3$)(C$_6$H$_{11}$NH$_2$)Cl$_2$] (**1**), a major metabolite of a recently developed, orally administered derivative. The bifunctional mixed amine complex **7** and a monofunctional triamine complex, *trans*-[Pt(NH$_3$)$_2$(4-aminoTEMPO)Cl]NO$_3$ (**8**), were synthesized to provide localized unpaired electron spin density for use in NMR spectral studies of their polynucleotide adducts. Compounds **7** and **8** readily coordinate to the N(7) positions of guanosine nucleosides, as revealed by ^{1}H, ^{31}P, and ^{195}Pt NMR spectroscopy. The NMR spectra were selectively broadened owing to distance-dependent relaxation from the unpaired electron localized on the nitroxyl radical of the 4-aminoTEMPO ligand. Platination of d(GpG) by the mixed amine complex **7** afforded two orientational isomers which differed with respect to the positioning of the 4-aminoTEMPO group toward either the 3′ or 5′ side of the phosphodiester linkage. The purified orientational isomers were readily distinguished by selective broadening of the ^{1}H NMR resonances of the 3′ and 5′ deoxyribose rings. The minimum energy solution structure for the 5′ orientational isomer of the platinated dinucleotide *cis*-[Pt(NH$_3$)(4-aminoTEMPO){d(GpG)}]$^+$ (**13**) was determined by NMR methods including combined diamagnetic (*J* coupling constants) and paramagnetic (electron-^{1}H, ^{31}P distances) constraints. Moreover, with the paramagnetic spin probe, we have been able to obtain the first observable NMR distance constraints for determining the configuration of the ζ or α torsion angles in any oligonucleotide. Dynamics trajectories (200 ps) for **13** demonstrated that only computations including paramagnetic distance constraints could determine the ζ$^-$, α$^-$ conformation of the phosphodiester linkage and the conformation of the 4-aminoTEMPO ligand. These NMR data and computational methods demonstrate the utility of long-range paramagnetic distance constraints in elucidating the NMR solution structures of DNA modified by cisplatin analogues.

Introduction

The anticancer drug *cis*-diamminedichloroplatinum(II) (cisplatin or *cis*-DDP) derives its biological activity from binding to deoxyribonucleic acid (DNA).[1−3] In the predominant adducts formed when cisplatin binds to DNA, the chloride ligands are replaced by new bonds to the N(7) positions of adjacent purine nucleotides from the same strand. Several methods have been used to identify structural changes that occur in DNA modified by cisplatin. X-ray crystallography and solution nuclear magnetic resonance (NMR) spectroscopy have characterized the head-to-head orientation of the two purine rings, the change in the 5′ deoxyribose ring pucker from C$_{2'}$ endo (S) to C$_{3'}$ endo (N), and hydrogen bonding of the ammine ligand on the 5′ side of the adduct with the backbone phosphate.[4−6] Alterations in the secondary structure of duplex DNA beyond the platinated nucleotides have not been well characterized either by X-ray crystallography or NMR spectroscopy.[47]

The difficulty in determining high-resolution NMR structures of double-stranded DNA is an inherent lack of measurable long-range distance constraints. The $1/r^6$ distance-dependent dipolar coupling between nuclear spins, measured by the nuclear Overhauser effect (nOe), is the primary NMR spectroscopic tool for determining three-dimensional structures of oligonucleotides in solution.[7] Proton nOe's fall off rapidly when the internuclear separation is greater than 5 Å, and values less than this limit correspond only to distances between protons within a single nucleotide, between adjacent base-stacked nucleotides, and between hydrogen bonded base pairs in DNA duplexes. The lack of nOe distance constraints between protons separated by more than one nucleotide leaves DNA duplex helical parameters, including roll, propeller-twist, and base slide, largely underdetermined.[8]

Several attempts have been made to elucidate the solution structure of a cisplatin-modified DNA duplex by using NMR spectroscopy.[9,10] Although claims of cisplatin-induced "bent"

[⊗] Abstract published in *Advance ACS Abstracts,* October 1, 1995.

(1) Bruhn, S. L.; Toney, J. H.; Lippard, S. J. *Prog. Inorg. Chem.* **1990**, *38*, 477−561.

(2) Sundquist, W. I.; Lippard, S. J. *Coord. Chem. Rev.* **1990**, *100*, 293−322.

(3) Reedijk, J. In *NMR Spectroscopy in Drug Research*; Jaroszewski, J. W., Schaumburg, K. and Kofod, H., Eds.; Munksgaard: Copenhagen, 1988; pp 341−357.

(4) Sherman, S. E.; Gibson, D.; Wang, A. H. J.; Lippard, S. J. *J. Am. Chem. Soc.* **1988**, *110*, 7368−7381.

(5) Admiraal, G.; van der Veer, J. L.; de Graaff, R. A. G.; den Hartog, J. H. J.; Reedijk, J. *J. Am. Chem. Soc.* **1987**, *109*, 592−594.

(6) den Hartog, J. H. J.; Altona, C.; Chottard, J. C.; Girault, J. P.; Lallemand, J. Y.; de Leeuw, F. A. A. M.; Marcelis, A. T. M.; Reedijk, J. *Nucl. Acids Res.* **1982**, *10*, 4715− 4730.

(7) van de Ven, F. J. M.; Hilbers, C. W. *Eur. J. Biochem.* **1988**, *178*, 1−38.

(8) Ulyanov, N. B.; Gorin, A. A.; Zhurkin, V. B.; Chen, B. C.; Sarma, M. H.; Sarma, R. H. *Biochemistry* **1992**, *31*, 3918−3930.

(9) den Hartog, J. H. J.; Altona, C.; Van Boom, J. H.; van der Marel, G. A.; Haasnoot, C. A. G.; Reedijk, J. *J. Biomol. Struct. Dyn.* **1985**, *2*, 1137.

0002-7863/95/1517-10702$09.00/0

or "kinked" DNA duplexes were made on the basis of these studies, the derived structures included the results of molecular mechanics and dynamics calculations that were not constrained by the NMR data. Determination of a DNA duplex with a bent or kinked helical conformation from nOe data alone is risky, since only a small subset of nOe's located at the site of the platinum cross-link are available to constrain the conformation of the helix. In the absence of such constraints, the predominant energy term in fixing cisplatin-modified DNA must come from the force field parametrization of platinum–nucleotide interactions. Recently, the structures of a DNA hairpin stabilized by ethylenediaminedichloroplatinum(II), [Pt(en)Cl_2], and of a cisplatin-modified DNA duplex with a d(G*pTpG*) cross-link were determined from NMR-constrained refinement.[11,12] For both of these models, only nOe NMR data were used to refine the platinated complexes, and therefore the structures may suffer from model and force field bias.

To determine accurately a platinum-modified duplex DNA conformation by NMR spectroscopy, it would be necessary to have many distance relationships between nucleotides across the DNA helix (>9 Å between deoxyribose rings) and between nucleotides on the same strand separated by two or more bases (10–20 Å). One method for providing these long-range constraints is through distance-dependent paramagnetic NMR relaxation effects. Both nitroxyl radicals and paramagnetic transition metal ions have been used for such long-range distance measurements in macromolecules,[13–18] with the greater magnetic moment of the electron expanding the range for $1/r^6$ dipolar electron–nuclear interactions to 30 Å.

In order to provide such a source of local paramagnetism for NMR structural studies of platinated DNA, we have employed the 4-aminoTEMPO ligand, previously used to prepare cisplatin analogues containing nitroxide ligands (Chart 1).[19,20] Electron paramagnetic resonance (EPR) spectroscopy demonstrated that these paramagnetic cisplatin analogues readily form complexes with oligonucleotides. Since the mixed amine–cyclohexylamine complex *cis*-[Pt(NH_3)($C_6H_{11}NH_2$)Cl_2] (**1**), a major metabolite of the Pt(IV) complex *cis,trans,cis*-[Pt(NH_3)(C_6H_{11}-NH_2)($OC(O)CH_3$)$_2Cl_2$] (**2**)[21] currently undergoing clinical trials, binds DNA in a manner similar to cisplatin,[22] we decided to investigate *cis*-amine(4-aminoTEMPO)chloroiodoplatinum(II) (**7**) (Chart 1) as a paramagnetic analogue to provide the desired long-range NMR distance constraints in platinum-modified DNA. The ability to reduce the nitroxyl radical conveniently to its diamagnetic hydroxylamine form and to obtain high-resolution NMR data on this form further contributed to the utility of this approach.

Chart 1

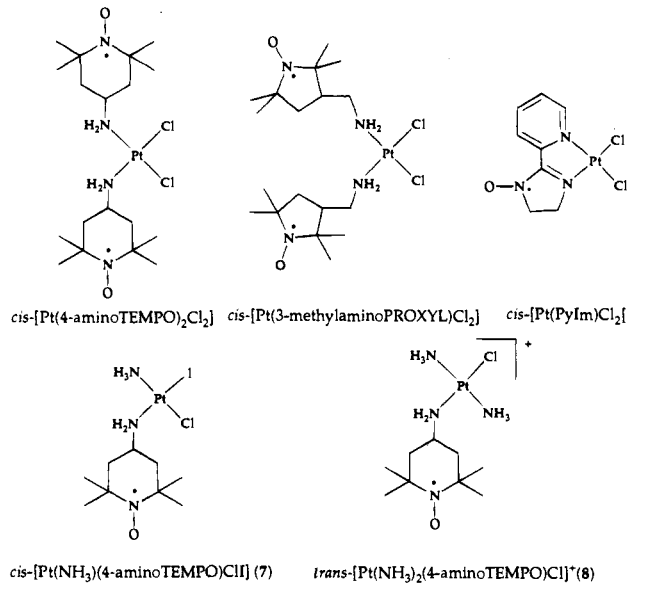

In this initial report, we present the synthesis and spectroscopic characterization of **7** and its adducts with 5′-GMP and d(GpG). Computational methods demonstrate that the paramagnetic NMR relaxation effects provide sufficient information for a detailed description of the local and long-range structural order in the d(GpG) platinum cross-link. These spectroscopic and computational results validate the application of paramagnetic NMR methodology for determining high-resolution structures of platinum-modified oligonucleotides in solution, opening the door to studies of larger and more complex molecules.

Experimental Section

Materials. The complexes *cis*-[Pt(NH_3)($C_6H_{11}NH_2$)Cl_2] (**1**) and *cis*- and *trans*-[Pt(NH_3)$_2Cl_2$] (**3**, **4**) were provided by the Johnson Matthey AESAR/Alfa Co., and (PPh_4)[Pt(NH_3)Cl_3] (**5**) and *cis*-[Pt(NH_3)(C_6H_{11}-NH_2)ClI] (**6**) were prepared by published methods.[21,23] Guanosine 5′-monophosphate (5′-GMP), 2′-deoxyguanosine 5′-monophosphate (5′-dGMP), phenylhydrazine, ascorbic acid, sodium 2,2-dimethyl-2-silapentane 5-sulfonate (DSS), 4-hydroxy-2,2,6,6-tetramethylpiperidinyloxy (TEMPOL), and 4-amino-2,2,6,6-tetramethylpiperidinyloxy (4-aminoTEMPO) were used as received from Sigma or Aldrich. Hydrated sodium d(GpG) was prepared by a solution phase β-(cyanoethyl)phosphoramidite method.[24]

Preparation of Platinum Complexes. Synthesis of *cis*-[Pt(NH_3)(4-aminoTEMPO)ClI] (7). This complex was prepared by a modification of the method previously described for synthesizing mixed amine platinum complexes.[21,23] A 0.147 g (0.236 mmol) amount of (PPh_4)[Pt(NH_3)Cl_3], (PPh_4)**5**, was suspended in 20 mL of methanol. A 3 mL portion of a methanol solution containing 0.0807 g (0.236 mmol, 1 equiv) of Na(BPh_4) was added and the solution was stirred for 10 min. The white precipitate of (PPh_4)(BPh_4) was centrifuged from the yellow supernatant. Next, 5 mL of H_2O was added to the methanol solution of Na[Pt(NH_3)Cl_3], (Na)**5**, and the methanol was removed under reduced pressure. A 0.0707 g (0.472 mmol, 2 equiv) portion of NaI dissolved in 2 mL of H_2O was added to the resulting aqueous solution of (Na)**5**. Immediately following NaI addition, 0.0444 g (0.259 mmol, 1.2 equiv) of 4-aminoTEMPO was added in 1 mL of H_2O. The yellow solution deposited a yellow brown solid over 6 h at 23 °C in the dark. The solid was collected and washed with 30 mL of H_2O and 10 mL of methanol. *cis*-[Pt(NH_3)(4-aminoTEMPO)ClI] (**7**) was obtained as a light yellow-brown solid (0.054 g, 42%). Anal. Calcd for $PtC_9H_{22}N_3O$ClI: C, 19.81; H, 4.06; N, 7.70. Found: C, 20.45; H, 4.65; N, 7.60. UV (λ_{max}, ethanol, nm): 220, 238 (sh). IR (KBr, cm^{-1}): 3199, 2974,

(10) Herman, F.; Kozelka, J.; Stoven, V.; Guittet, E.; Girault, J.-P.; Huynh-dinh, T.; Igolen, J.; Lallemand, J.-Y.; Chottard, J.-C. *Eur. J. Biochem.* **1990**, *194*, 119–133.
(11) Van Garderen, C. J.; Van Houte, L. P. A. *Eur. J. Biochem.* **1994**, *225*, 1169–1179.
(12) Iwamoto, M.; Mukundan, S.; Marzilli, L. G. *J. Am. Chem. Soc.* **1994**, *116*, 6238–6244.
(13) Yu, L.; Meadows, R. P.; Wagner, R.; Fesik, S. W. *J. Magn. Res. Ser. B* **1994**, *104*, 77–80.
(14) Girvin, M. E.; Fillingame, R. H. *Biochemistry* **1994**, *33*, 665–674.
(15) Rehmann, J. P.; Barton, J. K. *Biochemistry* **1990**, *29*, 1710–1717.
(16) Kosen, P. A. *Methods Enzymol.* **1989**, *177*, 86–121.
(17) Frederick, A. F.; Kay, L. E.; Prestegard, J. H. *FEBS Lett.* **1988**, *238*, 43–48.
(18) Schmidt, P. G.; Kuntz, I. D. *Biochemistry* **1984**, *23*, 4261–4266.
(19) Mathew, A.; Bergquist, B.; Zimbrick, J. *J. Chem. Soc., Chem. Commun.* **1979**, 222–224.
(20) Mastin, S. H. *Varian Instruments Application Note* **1975**, *EPR-75-1*, 1–14.
(21) Giandomenico, C. M.; Abrams, M. J.; Murrer, B. A.; Vollano, J. F.; Rheinheimer, M. I.; Wyer, S. B.; Bossard, G. E.; Higgins, J. D. *Inorg. Chem.* **1995**, *34*, 1015–1021.
(22) Hartwig, J. F.; Lippard, S. J. *J. Am. Chem. Soc.* **1992**, *114*, 5646.
(23) Abrams, M. J.; Giandomenico, C. M.; Vollano, J. F.; Schwartz, D. A. *Inorg. Chim. Acta* **1987**, *131*, 3–4.
(24) Sugden, K. Personal Communication.

2930, 1559, 1243 cm^{-1}. ^1H NMR (DMF-d_7, 300 MHz): δ 1.12, (s, 12 H), 1.46 (dd, 2 H), 2.37 (dd, 2 H), 3.37 (m, 1 H), 4.23 (bs, 3 H), 4.96 (bs, 2 H), 6.5−8.5 (phenylhydrazine protons). ^{195}Pt NMR (DMF-d_7, 64.347 MHz): δ −2662. EPR (H_2O): g 2.0064 (t, A = 16.956 G).

Synthesis of *trans*-[Pt(NH$_3$)$_2$(4-aminoTEMPO)Cl]NO$_3$ (8). A suspension of 0.985 g (0.328 mmol) of *trans*-[$Pt(NH_3)_2Cl_2$] (**4**) and 0.056 g (0.327 mmol, 1 equiv) of $AgNO_3$ in 5 mL of DMF was stirred for 18 h and the precipitated AgCl was removed by centrifugation. A 0.056 g (0.327 mmol, 1 equiv) portion of 4-aminoTEMPO was added to the activated platinum complex in 1 mL of DMF. The DMF reaction mixture was stirred for 6 h at 23 °C and solvent was removed under reduced pressure. The yellow solid **8** was washed with 20 mL of ice-cold ethanol and ether and recrystallized as a yellow-brown powder from H_2O (0.118 g, 77%). Anal. Calcd for $PtC_9H_{25}N_5O_4Cl$: C, 21.71; H, 5.06; N, 14.07. Found: C, 22.61; H, 5.24; N, 13.93. UV (λ_{max}, ethanol, nm): 206, 248 (sh). IR (KBr, cm^{-1}): 3204, 2982, 1652, 1613, 1389, 1367, 1332, 1242 cm^{-1}. ^1H NMR (DMF-d_7, 300 MHz): δ 1.12 (s, 12 H), 1.45 (dd, 2 H), 2.29 (dd, 2 H), 3.19 (m, 1 H), 4.25 (bs, 6 H), 5.5 (bs, 2 H), 6.5−8.5 (phenylhydrazine protons). ^{195}Pt NMR (DMF-d_7, 64.347 MHz): δ −2444. EPR (H_2O): g 2.0064 (t, A = 16.956 G)

Mononucleotide Adducts. Solutions of *trans*-[$Pt(NH_3)_2$(4-aminoTEMPO)X]NO_3 (X = DMF, NO_3) and *cis*-[$Pt(NH_3)$(4-aminoTEMPO)X_2] (X = DMF, NO_3^-) in DMF-d_7 were prepared by allowing *trans*-[$Pt(NH_3)_2$(4-aminoTEMPO)Cl]NO_3 (**8**) to react with 0.98 equiv of $AgNO_3$ or *cis*-[$Pt(NH_3)$(4-aminoTEMPO)ClI] (**7**) to react with 1.98 equiv of $AgNO_3$ at 23 °C for 18 h in the dark. Following centrifugation of precipitated AgCl and/or AgI, the supernatant was added to a D_2O solution containing an excess of the desired nucleotide. Progress of the reactions was followed by ^1H NMR spectroscopy and absorbance at 260 nm in reversed phase HPLC chromatograms.

***trans*-[Pt(NH$_3$)$_2$(4-aminoTEMPO)(5′-GMP)] (9).** A D_2O solution of 5′-GMP was allowed to react with a DMF-d_7 solution of *trans*-[$Pt(NH_3)_2$(4-aminoTEMPO)X]NO_3 (X = DMF, NO_3^-) for 24 h at 23 °C. The D_2O solution containing *trans*-[$Pt(NH_3)_2$(4-aminoTEMPO)(5′-GMP)] (**9**) was reduced in situ with 2 mol equiv of ascorbic acid before collecting NMR spectra; compound **9** was not isolated. ^1H NMR of the product mixture (D_2O, 300 MHz): δ 1.15 (s, 12 H), 1.51(dd, 2 H), 2.40 (dd, 2 H), 3.10 (m, 1 H), 3.80−4.42 (overlapping ribose and ascorbic acid protons), 5.81 (d, 1 H), 8.65 (s, 1 H). ^{195}Pt NMR (D_2O, 64.347 MHz): δ −2576.

***trans*-[Pt(NH$_3$)$_2$(4-aminoTEMPO){5′-d(GMP)}] (10).** This complex was prepared from a D_2O solution of 5′-d(GMP) and a DMF-d_7 solution of *trans*-[$Pt(NH_3)_2$(4-aminoTEMPO)X]NO_3 (X = DMF, NO_3). Compound **10** was collected from a C-18 reversed phase HPLC column at 12 min into a linear gradient (20 min) of 95:5 (A:B, defined below) to 90:10 and lyophilized to dryness (yield, 34%). The hydroxylamine complex was prepared by allowing a 5-fold molar excess of ascorbic acid to react with **10** in water for 20 min at 23 °C. The excess ascorbic acid was removed by ion exchange chromatography, and aqueous solutions of the nitroxide and hydroxylamine forms of **10** were lyophilized to dryness to afford white solids. ^1H NMR (D_2O, 500 MHz): Table S1, supporting information. EPR (H_2O): g 2.0063 (t, A = 16.958 G).

***cis*-[Pt(NH$_3$)(4-aminoTEMPO)(5′-GMP)$_2$]$^{2-}$ (11).** A solution of *cis*-[$Pt(NH_3)$(4-aminoTEMPO)X_2] (X = DMF, NO_3^-) in DMF-d_7 was allowed to react with a D_2O solution containing 3 mol equiv of 5′-GMP. The hydroxylamine complex was prepared by reduction in situ with 2 equiv of ascorbic acid, and the resulting *cis*-[$Pt(NH_3)$(4-aminoTEMPO)(5′-GMP)$_2$]$^{2-}$ (**11**) was not isolated. ^1H NMR (D_2O 300 MHz): δ 1.19 (s, 6 H), 1.21 (s, 6 H), 1.8 (dd, 2 H), 2.55 (m, 2 H), 2.75 (m, 1 H), 3.90-4.7 (overlapping resonances from ribose and ascorbic acid), 5.8 (m, 2 H), 8.5 (s, 1 H), 8.7 (s, 1 H). ^{195}Pt NMR (D_2O, 64.347 MHz): δ −2483.

Dinucleotide Adducts. *cis*-[Pt(NH$_3$)(4-aminoTEMPO){d(GpG)}]$^+$, 3′ and 5′ Orientational Isomers (12, 13). A solution of *cis*-[$Pt(NH_3)$(4-aminoTEMPO)X_2] (X = DMF, NO_3^-) was prepared by allowing 0.054 g of *cis*-[$Pt(NH_3)$(4-aminoTEMPO)ClI (**7**) (0.099 mmol) and 0.033 g of $AgNO_3$ (0.194 mmol, 1.98 equiv) to react in 1 mL of DMF with vigorous shaking at 23 °C for 18 h in the dark. Following centrifugation of precipitated AgCl and AgI, the DMF solution of activated **7** was diluted with 20 mL of H_2O and the pH was adjusted to 4.6 with 0.01 M NaOH. A 1 μM aqueous solution of Na[d(GpG)] (0.0673 g/20 mL, 0.109 mmol) was prepared, and the pH of the solution was adjusted to 4.6 with 0.01 M HNO_3. The solutions of *cis*-[$Pt(NH_3)$(4-aminoTEMPO)X_2] and d(GpG) were combined and stirred for 48 h at 23 °C. Several preparations formed a purple paramagnetic precipitate which was separated by centrifugation. Preparative C-18 reversed phase HPLC under isocratic conditions of 88:12 (A:B, defined below) was used to purify the two orientational isomers of *cis*-[$Pt(NH_3)$(4-aminoTEMPO){d(GpG)}]$^+$, **12**, which eluted at 17 min, and **13**, which eluted at 22 min. The hydroxylamine derivatives of **12** and **13** were prepared at 23 °C by reduction with 5 mol equiv of ascorbic acid for 20 min, followed by anion exchange chromatography. Repeated lyophilization of solutions containing nitroxide or hydroxylamine complexes gave white solids which readily dissolved in H_2O. ^1H NMR (D_2O 500 MHz): **12**, Table S2, supporting information; **13**, Table 1. EPR (H_2O): **12**, g 2.0064 (t, A = 16.956); **13**, g 2.0063 (t, A = 16.958 G). MS: **13** Calcd for $PtC_{29}H_{47}N_{13}O_{11}P$: m/z, 979.29. Found: M^+, 979.2; $M^+(-NH_3)$, 962.5; M^+(-4-aminoTEMPO), 808.8.

Physical Methods

NMR spectra were recorded on Varian UNITY 300 and 500 MHz spectrometers. Paramagnetic nitroxides were reduced with ascorbic acid in D_2O or phenylhydrazine in DMF-d_7 to form the diamagnetic hydroxylamine complexes. Nitroxide reduction was followed by the appearance of methyl proton resonances for the 4-aminoTEMPO ligand in the ^1H NMR spectrum. Excess ascorbic acid was removed by anion exchange chromatography over DEAE Sephadex in the acetate form. Integratable ^1H NMR spectra were typically obtained by using 8000 Hz spectral width and 10 s delays between 90° pulses of 15 μs. ^1H NMR spectra were internally referenced to partially deuterated solvent at 2.74 ppm for DMF-d_7 and to DSS at 0 ppm for D_2O. ^{195}Pt NMR spectra were externally referenced to 0.1 M $K_2[PtCl_4]$ in 1 M HCl at −1624 ppm. ^{31}P NMR spectra were externally referenced to 85% phosphoric acid at 0 ppm. Nonselective one-dimensional (1-D) T_1 and T_2 NMR relaxation data were obtained with an inversion recovery pulse sequence[25] and the Carr−Purcell−Meiboom−Gill (CPMG)[26] method, respectively, and the relaxation data were fit to exponential decays.[27] ^1H NMR J-coupling constants for the hydroxylamine complexes were determined from extensive 1-D homonuclear decoupling experiments at 50 °C. J-coupling NMR data were resolution enhanced by Gaussian weighting prior to Fourier transformation. Magnitude COSY NMR spectra were accumulated with 2048 F_2 × 256 F_1 data points at a spectral width of 5000 Hz, a 90°, 90° pulse sequence, and presaturation of residual HDO signal during a preacquisition delay of 1 s. Data were zero-filled to 1024 points in F_1, and both F_1 and F_2 dimensions were weighted with sine-squared window functions before Fourier transformation.

EPR spectra were obtained at 23 °C with a Bruker ESP-300 spectrometer operating in the X-band range at 9.38 GHz. Spectra were externally referenced to a 1 mM aqueous sample of TEMPOL (g = 2.0062). Samples were dissolved in 80 μL of H_2O and transferred to a 100 μL glass capillary in a 5 mm quartz EPR tube. Spectra were typically accumulated with a center field of 3340 G, 150 G sweep width, 1.0 G modulation amplitude, 25 kHz modulation frequency, 164 ms time constant, and 1−2 mW of microwave power.

High-pressure liquid chromatographic (HPLC) traces were obtained with reversed phase VYDAC C-18 columns running at 1 mL/min for analytical and 10 mL/min for preparative scales. A Waters-600E instrument was used to control solvent flow rates and gradients while recording the absorbance at 260 nm on a Waters-486 detector. Buffers for HPLC consisted of 0.1 M ammonium acetate adjusted to pH 6.4 with acetic acid (buffer A) and a 50/50 mixture of buffer A and acetonitrile (buffer B).

Ultraviolet and visible (UV−vis) spectra were obtained in 1 cm path length cells on a Hewlett Packard 8452A diode array or Perkin-Elmer Lambda 7 spectrophotometer. Calculated molar extinction coefficients (M^{-1} cm^{-1}) were used for determining nucleotide concentrations as follows: d(GpG) = 21 600; 5′-d(GMP), 5′-GMP = 11 500.[28]

(25) Vold, R. L.; Waugh, J. S.; Klein, M. P.; Phelps, D. E. *J. Chem. Phys.* **1968**, *48*, 3831− 3832.
(26) Meiboom, S.; Gill, D. *Rev. Sci. Instrum.* **1958**, *29*, 688.
(27) Varian *VNMR 4.1* 1989−1992.

Platinum atomic absorption spectra were obtained on a Varian GTA-95 spectrophotometer equipped with a graphite furnace. All samples were compared to a standard curve established from a solution of K_2PtCl_6.

Solution pH measurements were obtained with an Orion Research-960 instrument operating with an Ingold combination pH microelectrode. Solution pH values were adjusted with 0.01 M solutions of NaOH or HNO_3. NMR pH titrations were obtained by measuring pD and are uncorrected for the deuterium isotope effect. NMR solution pD was adjusted with 10% solutions of NaOD and DCl.

Mass spectral analyses were determined on an Applied Biosystems BIO-ION 20 instrument after ionization by plasma desorption using a ^{252}Cf source.

Unbuffered samples (pH 7.0 ± 0.2) used for paramagnetic distance measurements were lyophilized twice from 99.99% D_2O, and the final sample concentration was adjusted to 1 mM in order to minimize intermolecular paramagnetic relaxation (vide infra). Sample concentrations were determined by UV−vis and platinum atomic absorption spectroscopy.

Structure Determination

Paramagnetic Distance Constraints. The NMR relaxation rate, T_{obs}^{-1}, for a paramagnetic molecule contains a sum of diamagnetic (T_{dia}^{-1}) and paramagnetic ($T_{paraintra}^{-1}$) relaxation rates (eq 1).[16] In order

$$\frac{1}{T_{obs}} = \frac{1}{T_{dia}} + \frac{1}{T_{paraintra}} + \frac{1}{T_{parainter}} \quad (1)$$

to determine the T_{dia}^{-1} component of T_{obs}^{-1}, the nitroxyl radical was converted to the diamagnetic hydroxylamine and T_{dia}^{-1} was readily determined by conventional high-resolution NMR methods. $T_{paraintra}^{-1}$ was obtained by subtracting T_{dia}^{-1} from T_{obs}^{-1} in the absence of intermolecular paramagnetic relaxation ($T_{parainter}^{-1}$).

Three sets of nonselective T_1 and T_2 relaxation times were determined from 1-D ^1H (500 MHz) and ^{31}P (202 MHz) NMR spectra for the nitroxide and hydroxylamine complexes. T_{1para} and T_{2para} were determined for each proton from eq 1.[16] In order to determine the distance from the electron to the proton, the correlation time must be measured for each electron−proton vector ($\tau_{c\ e\text{-}n}$), eq 2. The ratio of (T_{1para}^{-1}/

$$\frac{1}{\tau_{c\ e\text{-}n}} = \frac{1}{\tau_{c\ \text{rotational molecule}}} + \frac{1}{\tau_{c\ \text{relaxation electron}}} \quad (2)$$

T_{2para}^{-1}), eq 3, for each proton resonance was used to determine the correlation time for each unique electron−proton vector ($\tau_{c\ e\text{-}n}$), eq 2.[16] By incorporating the errors in determining T_{1para} and T_{2para} into eq 3, upper and lower bounds for $\tau_{c\ e\text{-}n}$ were established (Table 1). In eq 3 τ_{c1} and ω_I are the correlation time and the Larmour frequency for the nucleus, respectively, and τ_{c2} and ω_s are the respective correlation time and Larmour frequency for the electron.

$$\frac{T_{1para}^{-1}}{T_{2para}^{-1}} = 2\left\{\frac{3\tau_{c1}}{1+\omega_I^2\tau_{c1}^2} + \frac{7\tau_{c2}}{1+\omega_s^2\tau_{c2}^2}\right\} \Bigg/ \left\{4\tau_{c1} + \frac{3\tau_{c1}}{1+\omega_I^2\tau_{c1}^2} + \frac{13\tau_{c2}}{1+\omega_s^2\tau_{c2}^2}\right\} \quad (3)$$

From $\tau_{c\ e\text{-}n}$, T_{1para}, T_{2para}, and their upper and lower bounds (1σ), distances (r) with errors between the electron (N_1 of 4-aminoTEMPO) and various nuclei in the molecule were calculated by using eqs 4 and 5.[29] In these equations, S is the total unpaired electron spin, γ_i is the

$$\frac{1}{T_{1para}} = \frac{2}{15}\frac{S(S+1)\gamma_I^2 g^2\beta^2}{r^6}\left\{\frac{3\tau_{c1}}{1+\omega_I^2\tau_{c1}^2} + \frac{7\tau_{c2}}{1+\omega_s^2\tau_{c2}^2}\right\} + \frac{2}{3}S(S+1)\left(\frac{A}{\hbar}\right)^2\left\{\frac{\tau_{c2}}{1+\omega_s^2\tau_{c2}^2}\right\} \quad (4)$$

$$\frac{1}{T_{2para}} = \frac{1}{15}\frac{S(S+1)\gamma_I^2 g^2\beta^2}{r^6}\left\{4\tau_{c1} + \frac{3\tau_{c1}}{1+\omega_I^2\tau_{c1}^2} + \frac{13\tau_{c2}}{1+\omega_s^2\tau_{c2}^2}\right\} + \frac{1}{3}S(S+1)\left(\frac{A}{\hbar}\right)^2\left\{\tau_{c1} + \frac{\tau_{c2}}{1+\omega_s^2\tau_{c2}^2}\right\} \quad (5)$$

gyromagnetic ratio for the nucleus, g is the electron g value, β is the Bohr magneton, A is the hyperfine coupling constant, $\hbar$ is Planck's constant divided by 2π, and τ_{c1}, τ_{c2}, ω_I, and ω_s are as previously described for eq 3. At high magnetic field strengths, terms in eqs 4 and 5 which include ω_s become insignificant because of the large magnetic moment of the electron. Electron (N_1 of 4-aminoTEMPO)-to-nuclear distance constraints were applied in CHARMm with a square well nOe potential (25 kcal/(mol·Å^2)) fixed by upper and lower bounds of the distance measurement (Table 1).

Torsional Constraints. NMR J-coupling constants were converted to torsion constraints by use of generalized Karplus equations for H−C−C−H[7,30] and H−C−O−P[7,31] with a force constant of 100 kcal/mol ϕ^2.

Model Building and Structure Refinement. Molecular mechanics and dynamics calculations were obtained with the computational program CHARMm[32] (Version 22) operating under QUANTA 4.0 (Molecular Simulations Inc.) on a Silicon Graphics Indigo-II Extreme workstation. Parameters for all stretching, bending, and torsional forces were adapted from previous molecular mechanics calculations for platinum compounds[10] and by fitting the vibrational spectra for $[Pt(NH_3)_4]^{2+}$ within the VIBRAN package of CHARMm (vide infra). Atomic charges were taken from the CHARMm 22 force field and modified for platinum binding at N(7) of guanosine.[33] Nonbonded interactions were scaled by a 4 Å radius-dependent dielectric and no solvent or counterions were included in the computations. Starting coordinates for the 5′ orientational isomer of *cis*-[Pt(NH$_3$)(4-aminoTEMPO){d(GpG)}]$^+$ (**13**) were obtained by docking a square-planar *cis*-[Pt(NH$_3$)(4-aminoTEMPO)] fragment to the N(7) sites of d(GpG) followed by energy minimization of the platinated complex to 0.01 kcal/mol with the adopted basis Newton−Raphson method. Molecular dynamics trajectories were prepared by heating to 300 K over 0.6 ps followed by an additional 0.6 ps of equilibration at 300 K. The SHAKE algorithm was used to constrain bond distances to hydrogen atoms during dynamics.[34] Dynamics trajectories were run for 200 ps at 300 K with updating of trajectories every 0.1 fs. Structural coordinates were obtained every 0.1 ps to follow conformational changes during dynamics. Structures were compared between dynamics trajectories either unconstrained (MM), constrained by torsional constraints (J), constrained by paramagnetic distances (NO), or constrained by a sum of paramagnetic and torsional constraints (J+NO).

A representative conformation from each trajectory was determined by averaging the coordinates over the last 2 ps of dynamics, followed by 100 cycles of minimization with the conjugate gradient method to remove nonbonded contacts.

Results and Discussion

Spin-Labeled Platinum Complexes. *trans*-[Pt(NH$_3$)$_2$(4-aminoTEMPO)Cl]NO$_3$ (8). The complex *trans*-[Pt(NH$_3$)$_2$(4-aminoTEMPO)Cl]$^+$(**8**) was prepared in high yield by allowing *trans*-[Pt(NH$_3$)$_2$ClX] (X = DMF, NO_3^-) to react with 4-ami-

(28) *Handbook of Biochemistry and Molecular Biology*, 3rd ed.; Fasman, G. D., Ed.; CRC Press: Cleveland, 1975; Vol. I.
(29) Solomon, I.; Bloembergen, N. *J. Chem. Phys.* **1956**, *25*, 261−266.
(30) Haasnoot, C. A. G.; De Leeuw, F. A. A. M.; De Leeuw, H. P. M.; Altona, C. *Recl. Trav. Chim. Pays Bas* **1979**, *28*, 567−577.
(31) Lankhorst, P. P.; Haasnoot, C. A. G.; Erkelens, C.; Altona, C. *J. Biomol. Struct. Dyn.* **1984**, *1*, 1387−1405.
(32) Brooks, R. B.; Bruccoleri, R. E.; Olafson, B. D.; States, D. J.; Swaminathan, S.; Karplus, M. J. *J. Comput. Chem.* **1983**, *4*, 187−217.
(33) Kozelka, J. Personal Communication.
(34) Ryckaert, J. P.; Ciccotti, G.; Berendsen, H. J. C. *J. Comp. Phys.* **1977**, *23*, 327−341.

Table 1. ^1H and ^{31}P NMR Assignments and Constraints for the 5′ Orientational Isomers of *cis*-[Pt(NH$_3$)(4-aminoTEMPO){d(GpG)}]$^+$ (**13**)[a]

resonance	δ (ppm)	J (Hz)	torsion angle (deg)	T_{1para} (s)	$\tau_{c\ en}$ (ns)	NO to ^1H, ^{31}P dist (Å)
3′-H$_8$	8.49			0.0191(8)	0.18(11)	7.3(6)
5′-H$_8$	8.32			0.0072(6)	*b*	6.2(5)[c]
3′-H$_{1'}$	6.19	6.1 to H$_{2''}$	42.1[d]	0.110(6)	0.35(8)	10.4(1)
		7.6 to H$_{2'}$				
5′-H$_{1'}$	6.25	7.2 to H$_{2''}$	−36.1	0.0023(1)	0.16(7)	7.6(4)
3′-H$_{3'}$	4.72	3.5 to H$_{4'}$	−128.2	0.30(3)	0.65(35)	11.8(3)
5′-H$_{3'}$	4.55	8.5 to H$_{4'}$	−160.4	0.021(1)	0.15(4)	7.5(3)
		7.0 to ^{31}P[e]	−34.3			
3′-H$_{4'}$	4.18	3.5 to H$_{5'}$/H$_{5''}$	56.8[e]	0.200(6)	0.37(9)	11.5(1)
		<2 to ^{31}P				
5′-H$_{4'}$	4.08	2.8 to H$_{5'}$	*d*	0.053(2)	0.45(6)	9.1(1)
3′-H$_{5'/5''}$	4.03	3.0 to ^{31}P	−54.0[e]	0.148(2)	0.34(9)	10.9(1)
5′-H$_{5'}$	3.87	12.7 to H$_{5''}$		0.0192(7)	0.26(17)	7.4(4)
5′-H$_{5''}$	3.57	4.2 to H$_{4'}$	62.8	0.0121(7)	0.20(12)	6.8(5)
3′-H$_{2''}$	2.77	14.0 to H$_{2'}$		0.065(2)	0.82(5)	9.0(1)
		6.4 to H$_{3'}$	−39.4			
5′-H$_{2'}$	2.57	14.0 to H$_{2'}$		0.032(2)	0.22(17)	7.7(8)
		7.3 to H$_{3'}$	37.2			
3′-H$_{2''}$	2.53	3.4 to H$_{3'}$	*d*	0.129(9)	0.43(14)	10.6(1)
5′-H$_{2''}$	2.72	10.7 to H$_{3'}$	*d*	*f*	*f*	*f*
PO$_4$	−0.35			0.38(3)	2.9(5)	10.0(2)
H$_a$	2.69	3.4 to H$_b$	57.9			
H$_b$[g]	2.22	12.5 to H$_c$				
H$_c$[g]	1.51	2.7 to H$_a$	62.5			
CH$_{3\ d}$[g]	0.98					
CH$_{3\ e}$[g]	0.90					

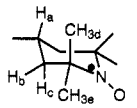

[a] Numbers in parentheses are errors at the ±1σ level. [b] S/N too low for determination of T_{2para}. [c] $\tau_{c\ en}$ used from 3′-H$_8$ resonance. [d] Duplicate torsional constraint; only one constraint/dihedral angle is allowed in CHARMm. [e] Obtained from ref 6. [f] Overlapping resonances prevent determination. [g] Stereospecific assignments of H$_b$, H$_c$, CH$_{3d}$, and CH$_{3e}$ were not obtained.

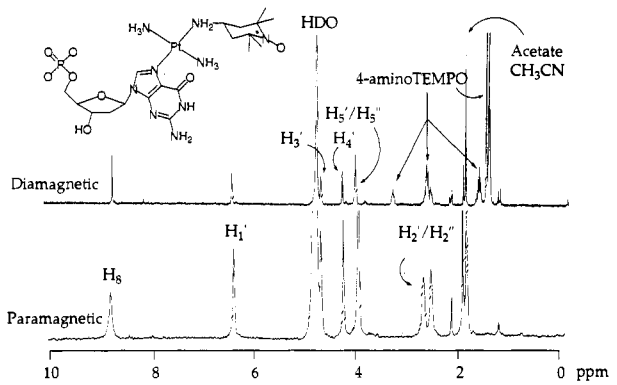

Figure 1. ^1H NMR spectra at 500 MHz for paramagnetic (oxidized) and diamagnetic (reduced) forms of *trans*-[Pt(NH$_3$)$_2$(4-aminoTEMPO)-{5′-d(GMP)}] (**10**) in D$_2$O.

noTEMPO in DMF solution. Elemental analysis confirmed the expected stoichiometry for **8** as the nitrate salt, and EPR spectra of **8** showed a characteristic triplet for coupling of the electron to ^{14}N ($S = 1$) of the nitroxide. When this moiety was reduced to the hydroxylamine with phenylhydrazine in DMF, the EPR spectrum displayed no signal at $g = 2$. The ^{195}Pt NMR spectrum for reduced **8** had a single resonance at −2444 ppm, 90 ppm upfield from that of [Pt(NH$_3$)$_3$Cl]$^+$ (−2354 ppm) and consistent with a PtN$_3$Cl coordination environment for Pt(II).[35] Integration of the ^1H NMR spectrum for reduced **8** confirmed the expected stoichiometry for the complex and revealed a 0.5 ppm downfield shift for the methine proton at the C$_4$ position of the 4-aminoTEMPO ligand, indicating coordination of the amine to the platinum.

***trans*-[Pt(NH$_3$)$_2$(4-aminoTEMPO)(nucleotide)], Nucleotide = 5′-GMP, 5′-d(GMP) (9, 10).** When *trans*-[Pt(NH$_3$)$_2$(4-aminoTEMPO)(X)] (X = DMF, NO$_3^-$) was allowed to react with 5′-GMP, the ^1H NMR spectrum of the reaction mixture revealed selective broadening for ^1H resonances of the 5′-GMP ligand. The downfield shifts of 0.6 ppm for the H$_8$ and 0.1 ppm for the H$_{1'}$ protons of 5′-GMP indicated platinum binding of a single nucleotide at the N(7) position of the guanosine.[36] The ^{195}Pt NMR spectrum of the hydroxylamine complex showed a single resonance at −2576 ppm, consistent with a Pt(II) complex with four coordinated nitrogen atoms.[35]

^1H NMR spectra of HPLC-purified nitroxide and hydroxylamine complexes of *trans*-[Pt(NH$_3$)$_2$(4-aminoTEMPO)(5′-d(GMP)], **10**, are shown in Figure 1. The paramagnetic nitroxide NMR spectrum exhibited distance-dependent broadening for the nucleotide resonances in **10** and the absence of ^1H resonances for the 4-aminoTEMPO ligand. The ^1H NMR spectrum for reduced **10** revealed sharp resonances for all nonexchangeable protons of the 5′-d(GMP) and the 4-aminoTEMPO ligand. The chemical shift similarity for oxidized and reduced 5′-d(GMP) protons of **10** indicated that contact shifts from the unpaired electron of the nitroxide are minimal and that reduction occurred selectively at the 4-aminoTEMPO ligand without converting Pt(II) to Pt(0). Homonuclear decoupling and a 2-D ^1H COSY spectrum of reduced **10** were used to assign the nonexchangable proton resonances, and nonselective T_1 and T_2 relaxation times for the nitroxide and hydroxylamine complexes were obtained to determine paramagnetic distances (Table S1, supporting information).

***cis*-[Pt(NH$_3$)(4-aminoTEMPO)Cl] (7).** This complex was prepared by a modification of the method used for synthesis of mixed *cis*-amine Pt complexes.[21,23] The generation of Na[Pt(NH$_3$)Cl$_3$] from Na(BPh$_4$) and (PPh$_4$)[Pt(NH$_3$)Cl$_3$] was a convenient method for preparing small batches of mixed *cis*-amine Pt complexes. The EPR spectrum of **7** exhibited the predicted three sharp lines. After reduction with phenylhydrazine, ^1H NMR spectra showed a downfield shift for the methine proton on the C$_4$ position of the 4-aminoTEMPO ligand, and spectral integrations confirmed the expected ^1H stoichiometry

(35) Pregosin, P. S. In *Annual Report on NMR Spectroscopy*; Academic Press Inc: London, 1986; Vol. 17; p 285.

(36) Lemaire, D.; Fouchet, M. H.; Kozelka, J. *J. Inorg. Biochem.* **1994**, *53*, 261−271.

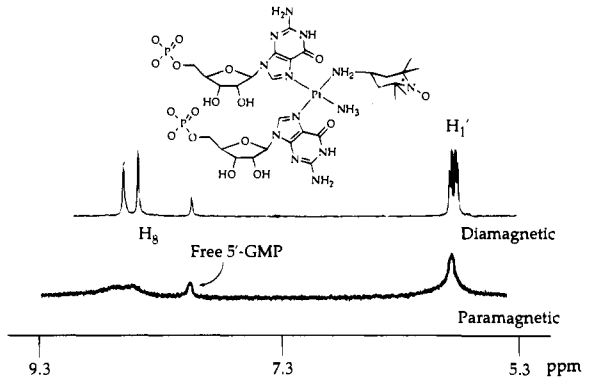

Figure 2. ^{1}H NMR spectra at 300 MHz for paramagnetic (oxidized) and diamagnetic (reduced) forms of *cis*-[Pt(NH_3)(4-aminoTEMPO)-(5′-GMP)$_2$]$^{2-}$ (**11**) in D_2O.

for **7**. A ^{195}Pt NMR spectrum for the hydroxylamine complex in DMF displayed a single resonance at −2662 ppm, a value consistent with that of −2653 ppm measured for *cis*-[Pt-(NH_3)($C_6H_{11}NH_2$)ClI], which we prepared by the methodology described.[21]

Conversion of **7** to the dichloro complex *cis*-[Pt(NH_3)(4-aminoTEMPO)Cl_2] (**14**) with 2 mol equiv of $AgNO_3$ followed by 0.1 M HCl resulted in significant reduction of the nitroxide to the hydroxylamine. A ^{195}Pt NMR spectrum for the hydroxylamine complex of **14** exhibited a single resonance at −2174 ppm. This resonance was 69 ppm upfield from the ^{195}Pt NMR resonance for *cis*-[Pt(NH_3)$_2Cl_2$] (-2105 ppm) and compared favorably to the −2157 ppm ^{195}Pt NMR resonance we observed for *cis*-[Pt(NH_3)($C_6H_{11}NH_2$)Cl_2] (**1**) in DMF. To prevent reduction of the 4-aminoTEMPO ligand, subsequent nucleotide binding reactions were carried out by activating the chloro/iodo complex **7** with silver nitrate in DMF.

***cis*-[Pt(NH_3)(4-aminoTEMPO)(nucleotide)$_2$]$^{2-}$, Nucleotide = 5′-GMP, 5′-d(GMP) (11).** When a DMF-d_7 solution containing *cis*-[Pt(NH_3)(4-aminoTEMPO)X_2] (X = DMF, NO_3^-) was added to a D_2O solution of 5′-GMP, the ^{1}H NMR spectra displayed two new broad, downfield-shifted H_8 resonances at 8.5 and 8.7 ppm. These observations were consistent with platinum coordination to the N(7) positions of two 5′-GMP nucleotides to form *cis*-[Pt(NH_3)(4-aminoTEMPO)(5′GMP)$_2$]$^{2-}$ (**11**). Ascorbic acid reduction of the nitroxide to the hydroxylamine revealed the expected ^{1}H NMR spectral changes associated with N(7) coordination (Figure 2). A ^{195}Pt NMR spectrum for reduced **11** exhibited a single resonance at −2483 ppm, which was consistent with PtN_4 coordination.[35,37]

Orientational Isomers of *cis*-[Pt(NH_3)(4-aminoTEMPO)-{d(GpG)}]$^+$ (12, 13). When *cis*-[Pt(NH_3)(4-aminoTEMPO)-(X_2] (X = DMF, NO_3^-) (**7**) was allowed to react with d(GpG) at pH 4.6, two predominant peaks were observed by reversed phase HPLC at 17 (**12**) and 22 (**13**) min (Figure 3A). These peaks were assigned to the orientational isomers that form when d(GpG) binds to an asymmetric *cis*-diamine Pt(II) complex (Chart 2).[22] One isomer has the 4-aminoTEMPO ligand adjacent to the 3′ nucleotide (cis to 3′ N(7)) of d(GpG), and the other isomer has the 4-aminoTEMPO ligand adjacent to the 5′-nucleotide (cis to 5′ N(7)) of d(GpG). Both **12** and **13** have a 3-line EPR spectrum at $g = 2$ (Figure 3B). The greater width of the upfield component in the EPR spectrum compared to that of the starting material **7** is caused by a decrease in the correlation time ($\tau_{c\ rotational}$) of **12** and **13**. A mass spectrum confirmed the expected molecular weight for **13** and revealed

(37) Bancroft, D. P.; Lepre, C. A.; Lippard, S. J. *J. Am. Chem. Soc.* **1990**, *112*, 6860−6871.

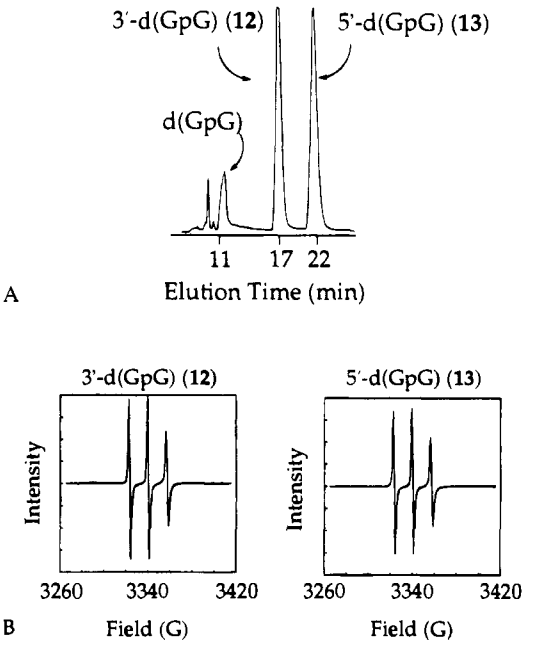

Figure 3. (A) HPLC chromatogram for the reaction of *cis*-[Pt(NH_3)-(4-aminoTEMPO)X_2] (X = H_2O, NO_3^-, DMF) and d(GpG) at pH 4.6 in H_2O. (B) EPR spectra of 3′ (**12**) and 5′ (**13**) orientational isomers of *cis*-[Pt(NH_3)(4-aminoTEMPO){d(GpG)}]$^+$ at 9.38 GHz and 298 K.

Chart 2

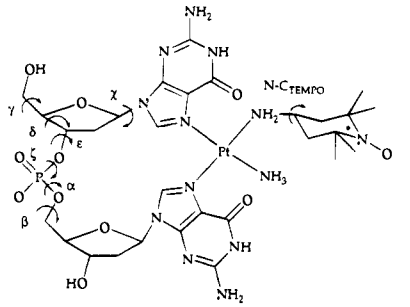

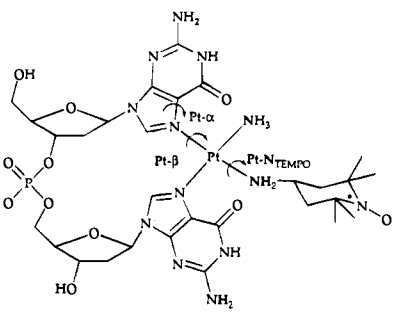

predominant fragments corresponding to loss of NH_3 or 4-aminoTEMPO ligands.

^{1}H NMR spectra of **12** and **13** in D_2O revealed a distance-dependent broadening for the nonexchangable protons. Following ascorbic acid reduction, pH dependent chemical shift titrations of the H_8 protons for **12** and **13** were obtained (Figure S1, supporting information). The chemical shifts for the H_8 protons of **12** and **13** did not significantly change below pH 8, indicating that the guanosine N(7) atoms were coordinated by platinum and unavailable for protonation. The change in chemical shift at pH > 8 was consistent with deprotonation at the N(1) position of the platinated guanosine rings.[36,38]

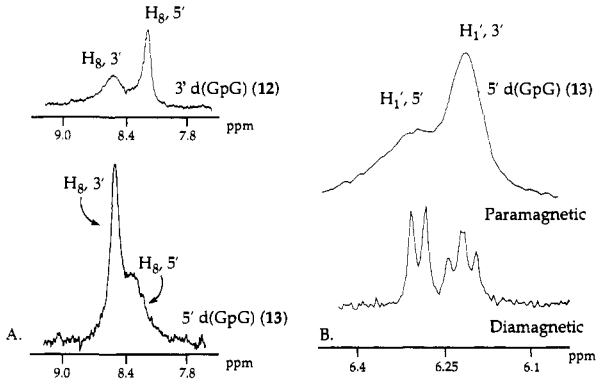

Figure 4. (A) ^{1}H NMR spectra of the H_8 protons for the paramagnetic (oxidized) 3′ (**12**) and 5′ (**13**) orientational isomers of *cis*-[Pt(NH$_3$)(4-aminoTEMPO){d(GpG)}]$^+$. (B) ^{1}H NMR spectra of the $H_{1'}$ protons for the diamagnetic (reduced) and paramagnetic (oxidized) 5′ orientational isomer of *cis*-[Pt(NH$_3$)(4-aminoTEMPO){d(GpG)}]$^+$ (**13**).

Previously, the assignment of 3′ and 5′ orientational isomers for *cis*-[Pt(NH$_3$)(C$_6$H$_{11}$NH$_2$){d(GpG)}]$^+$ complexes by NMR spectroscopy required enrichment in ^{15}N at the coordinated ammonia and N(7) positions of guanosine ligands.[22] For *cis*-[Pt(NH$_3$)(4-aminoTEMPO){d(GpG)}]$^+$, paramagnetic relaxation by the unpaired electron of the 4-aminoTEMPO ligand provided a simple method for determining the 3′ and 5′ orientational isomers by inspection of the ^{1}H NMR resonance line widths. In the absence of *J*-coupling, the NMR line width is a direct measurement of the T_2 relaxation time for the proton and thus is sensitive to the distance between protons and the unpaired electron.[16] The H_8 and $H_{1'}$ resonances are readily identified in ^{1}H NMR spectra for d(GpG)−platinum(II) complexes by their chemical shift values and *J*-coupling constants. In the d(GpG) ligand, the H_8 ^{1}H NMR resonance for the 5′-nucleotide is shifted upfield of the H_8 resonance for the 3′-nucleotide in single-stranded deoxyoligonucleotides,[39] and the $H_{1'}$ proton on the 5′-deoxyribose ring appears as a doublet because of the large *J*-coupling to the $H_{2''}$ proton when the deoxyribose ring is in the $C_{3'}$ endo conformation.[6,40] The $H_{1'}$ proton on the 3′-deoxyribose ring appears as collapsed doublet of doublets from *J*-coupling to both $H_{2'}$ and $H_{2''}$ protons when the deoxyribose ring is predominantly in the $C_{2'}$ endo conformation. Inspection of 1-D ^{1}H NMR spectra for the two isomers in the present study demonstrated that the upfield H_8 resonance of **12** had a significantly sharper line width than the downfield H_8 resonance (Figure 4). Conversely, the upfield H_8 resonance for **13** was broad and the downfield H_8 resonance was sharp. The chemical shifts of the H_8 resonances of **13** are concentration dependent. In 5 mM solutions, the sharp H_8 resonance of the 5′-nucleoside is farther upfield (Figure 4), but at 1 mM concentration the ^{1}H NMR spectrum reveals the broader, 5′-H_8 resonance to have shifted to downfield of the 3′-H_8 resonance. This shift in 5′-H_8 resonance position indicated alteration of the Pt-β torsion angles for **13** corresponding to an L_1-to-R_2 conformational change,[39] and reflecting intermolecular interactions in solutions more concentrated than 1 mM. Figure 4 also displays 1-D ^{1}H NMR spectra for the $H_{1'}$ resonances of **13** before and after reduction with ascorbic acid. These ^{1}H NMR spectra indicated that the $H_{1'}$ proton (doublet) on the 5′ deoxyribose ring is broadened more than the $H_{1'}$ proton on the 3′-deoxyribose ring. The differences in ^{1}H NMR line widths for the H_8 and $H_{1'}$ protons for **12** and **13** allowed the latter to be assigned as having the paramagnetic nitroxide adjacent to the 5′ end of the d(GpG) chelate, cis to 5′-N(7), and **12** as having the 4-aminoTEMPO ligand adjacent to the 3′ end of the d(GpG). An extensive study of ^{1}H NMR T_1 and T_2 relaxation times for all nonexchangable protons supported this simple assignment of the 3′ and 5′ orientational isomers from inspection of the ^{1}H NMR spectra (Figure 4, and Tables 1 and S2).

2-D COSY NMR spectra were obtained for the oxidized and reduced forms of both 3′ (**12**) and 5′ (**13**) orientational isomers of *cis*-[Pt(NH$_3$)(4-aminoTEMPO){d(GpG)}]$^+$. Sequential resonance assignments from reduced ^{1}H COSY spectra identified all nonexchangeable ^{1}H resonances in the two isomers (Tables 1 and S2). The absence of *J*-coupling between the $H_{1'}$ and $H_{2'}$ protons confirmed the assignment of the $H_{2'}$ and $H_{2''}$ protons on the 5′-deoxyribose ring and indicated that the 5′-deoxyribose sugar was primarily in a $C_{3'}$ endo conformation, as previously observed for other *cis*-diamineplatinum d(GpG) complexes.[6,40−43]

A concentration-dependent study of ^{1}H NMR T_1 relaxation times revealed that solutions of **13** more concentrated than 1 mM contained intermolecular contributions to the observed T_{1para} relaxation time (eq 1). Subsequently, therefore, NMR sample concentrations were adjusted to 1 mM before performing T_1 and T_2 relaxation measurements. The 1-D ^{1}H NMR spectra for the 3′ and 5′ orientational isomers had temperature-dependent changes in line width and resonance positions between 5 and 50 °C. T_{1para} and T_{2para} relaxation times were measured for the oxidized and reduced forms of **12** and **13** at 5 and 23 °C. Paramagnetic distances determined at both temperatures were the same within experimental error, but resonance overlap was minimal at 23 °C. Figure 5 summarizes in bar graph form the results of three independent determinations of T_{1para} relaxation times for **12** and **13** at 23 °C. For **13**, protons on the 5′-nucleotide clearly had much shorter relaxation times than the protons of the 3′-nucleotide, and within a single nucleotide the H_8, $H_{1'}$, $H_{2'}$, and $H_{2''}$ proton resonances were significantly closer to those of the 4-aminoTEMPO ligand than the $H_{3'}$ and $H_{4'}$ protons. A similar effect was observed for **12**, although fewer resonances were resolved in the 1-D ^{1}H NMR spectrum. The increased ^{1}H NMR spectral dispersion for **13** allowed for the determination of paramagnetic distances to all nonexchangeable protons except the 5′-$H_{2''}$. Resonance overlap for **12** limited the paramagnetic analysis to 10 of the 17 protons (Table S2). Subsequent analysis and computations were performed only on the 5′ orientational isomer **13** because of its highly resolved 1-D ^{1}H NMR spectrum.

An extensive NMR study of *cis*-[Pt(NH$_3$)$_2${d(GpG)}]$^+$ led to a solution structure model consistent with ^{1}H NMR *J*-coupling and ^{31}P chemical shift data.[6] Later studies of d(GpG) modified by the cisplatin analogues [Pt(dach)Cl$_2$], dach = (*R*,*R*)-, (*S*,*S*)-, (*R*,*S*)-cyclohexane-1,2-diamine, agreed with the *J*-coupling and ^{31}P chemical shift NMR data obtained for the cisplatin adduct[6] and suggested only a minor perturbation of the d(GpG) backbone.[43] The *J*-coupling constants (±1 Hz) determined in the present study for **13** (Table 1) were in close agreement with the NMR results for *cis*-[Pt(NH$_3$)$_2${d(GpG)}]$^+$, and suggested that d(GpG) backbone torsional angles are similar when chelated to cisplatin analogues.[22,41] ^{1}H NMR resonance overlap for the 3′-$H_{3'}$ proton of **13** and residual HDO protons prevented our

(38) Chottard, J. C.; Girault, J. P.; Chottard, G.; Lallemand, J. Y.; Mansuy, D. *J. Am. Chem. Soc.* **1980**, *102*, 5565−5572.
(39) Kozelka, J.; Fouchet, M. H.; Chottard, J. C. *Eur. J. Biochem.* **1992**, *205*, 895−906.
(40) Girault, J. P.; Chottard, G.; Lallemand, J. Y.; Chottard, J. C. *Biochemistry* **1982**, *21*, 1352−1356.
(41) Bloemink, M. J.; Heetebrij, R. J.; Inagaki, K.; Kidani, Y.; Reedijk, J. *Inorg. Chem.* **1992**, *31*, 4656−4661.
(42) den Hartog, J.; Altona, C.; van der Marel, G. D.; Reedijk, J. *Eur. J. Biochem.* **1985**, *147*, 371−379.
(43) Inagaki, K.; Nakahara, H.; Alink, M.; Kidani, Y. *Inorg. Chem.* **1990**, *29*, 4496−4500.

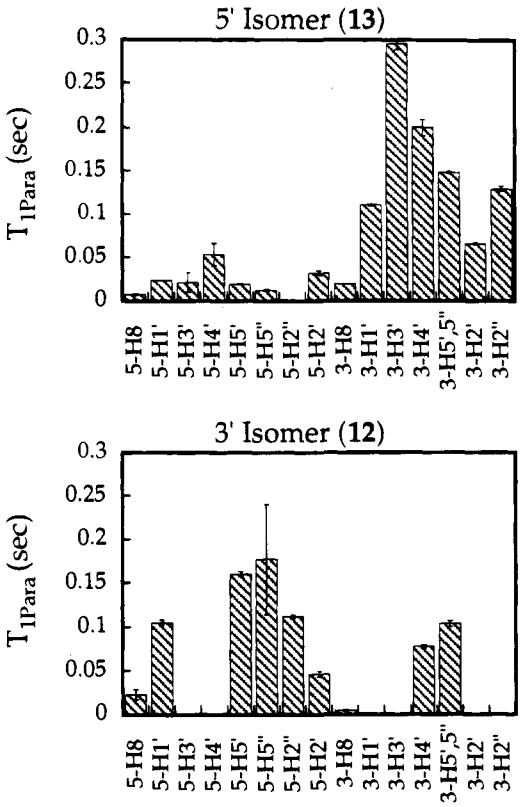

Figure 5. Bar graph showing the T_{1para} relaxation time for each proton in the 3′ (**12**) and 5′ (**13**) orientational isomers of *cis*-[Pt(NH$_3$)(4-aminoTEMPO){d(GpG)}]$^+$.

determination of an accurate ^{31}P−^{1}H *J*-coupling constant. Since our other *J*-coupling constants agree so closely with those for the *cis*-[Pt(NH$_3$)$_2${d(GpG)}]$^+$,[6] however, we used their ^{31}P−^{1}H *J*-coupling constant data to constrain the ϵ torsion angle.

Model Building and Refinement of the 5′ Orientational Isomer of *cis*-[Pt(NH$_3$)(4-aminoTEMPO){d(GpG)}]$^+$. The determination of structural properties from molecular mechanics methods often requires the addition of experimental constraints to obtain accurate structural models. Computations involving transition metals are particularly problematic because force field parameter development is still quite new and determining the electrostatic energy contribution for charged metal ions can be difficult. We present the analysis of our computational methods by examining the dynamics behavior of the complex for 200 ps at 300 K and by averaging the coordinates over the last 2 ps of dynamics. The dynamics behavior was particularly important in learning how experimental data limited the conformational freedom of the platinated dinucleotide. Since the dynamics trajectories did not include solvent molecules, the range of torsional motions observed is probably an upper limit.

New atom types and force field parameters were added to the CHARMm 22 force field to allow for the definition of the square-planar environment of Pt(II) (Table S4). Optimum bond angles for the 4-aminoTEMPO ligand were taken from the crystal structure analysis of a nickel(II) adduct[44] to maintain the geometry of the nitroxyl group (N−O) in the plane of the adjacent quaternary carbon atoms (C−N−C). The hydroxylamine form of the 4-aminoTEMPO ligand was used for all computations.

Comparison of the Refined Structures. Three constrained and one unconstrained structures of 5′-*cis*-[Pt(NH$_3$)(4-aminoTEMPO){d(GpG)}]$^+$ (**13**) were obtained from averaging the coordinates over the last 2 ps of the 300 K dynamics trajectories. A comparison of constrained and unconstrained complexes revealed several important features. All minimized structures were similar with respect to the positions of atoms comprising the Pt coordination sphere (RMSD, 0.094 Å), but there was little similarity for the other atoms of the molecule (RMSD all non-hydrogen atoms, 2.77 Å). The torsion angles (Chart 2) describing the four averaged structures of **13** together with those from X-ray crystallographic and NMR structure determinations of cisplatin-modified nucleotides containing d(GpG) are listed in Tables 2−4. Variations in torsion angles and pseudorotation parameters for **13** during 200 ps of dynamics at 300 K are shown as dials representations in Figure 6.

The dihedral angles for refinement of **13** unconstrained by NMR data (MM) sampled a very different region of conformational space than what has been observed experimentally by NMR spectroscopy and X-ray crystallography for cisplatin-modified d(GpG).[4-6] Most notably, the 3′-deoxyribose ring waspredominantly in the incorrect $C_{3'}$ endo conformation, and only for the 5′-deoxyribose ring and ϵ torsion angles did the

Table 2. Torsion Angles for 5′ Guanine of *cis*-Diamineplatinum(II) d(GpG) Complexes Derived from X-ray Crystal Structures and Molecular Mechanics Minimization with and without NMR Constraints[a]

	5′ nucleotide						
structure	*P*	ν_{max}	χ	γ	δ	Pt-α	Pt-β
J+NO d(GpG)	10	35	−89	71	89	−178	−127
J d(GpG)	20	34	−170	65	88	−177	−84
NO d(GpG)	12	40	−152	−67	80	−177	−74
MM d(GpG)	17	35	−140	175	86	−179	−97
d(pGpG) 1[b]	−12	33	−94(4)	56(4)	94(4)	−174	−108
d(pGpG) 2[b]	−8	35	−89(3)	65(4)	104(4)	−174	−110
d(pGpG) 3[b]	23	46	−138(4)	55(4)	91(5)	−178	−75
d(pGpG) 4[b]	27	48	−142(3)	36(6)	101(5)	−175	−75
d(CpGpG) 1[c]	14	34	−69(5)	48(5)	90(3)	−168	−140
d(CpGpG) 2[c]	−12	34	−76(4)	53(4)	97(3)	−176	−135
d(CpGpG) 3[c]	15	36	−74(7)	40(6)	88(3)	−163	−129
d(GpG)[d]	−1	37	−110	52	87		

[a] See Chart 2 for definition of torsion angles. [b] Reference 4, there are four crystallographically independent molecules. [c] Reference 5, there are three crystallographically independent molecules. [d] Reference 6, coordinates from NMR and model building.

Table 3. Torsion Angles for 3′ Guanine of *cis*-Diamineplatinum(II) d(GpG) Complexes Derived from X-ray Crystal Structures and Molecular Mechanics Minimization with and without NMR Constraints[a]

	3′ nucleotide						
structure	*P*	ν_{max}	χ	γ	δ	Pt-α	Pt-β
J+NO d(GpG)	120	39	−124	54	119	176	113
J d(GpG)	99	43	−111	64	104	179	123
NO d(GpG)	140	32	−121	52	133	177	123
MM d(GpG)	27	36	−112	−63	86	177	118
d(pGpG) 1[b]	84	38	−93(5)	30(11)	147(7)	168	105
d(pGpG) 2[b]	138	28	−110(4)	84(16)	108(15)	173	94
d(pGpG) 3[b]	130	49	−117(4)	47(8)	150(7)	−167	114
d(pGpG) 4[b]	136	43	−127(4)	42(7)	137(6)	−173	120
d(CpGpG) 1[c]	151	42	−116(6)	99(10)	107(3)	177	82
d(CpGpG) 2[c]	133	42	−91(5)	46(5)	127(4)	−176	83
d(CpGpG) 3[c]	174	36	−119(7)	189(10)	150(7)	166	98
d(GpG)[d]	149	34	−115	58	137		

[a] See Chart 2 for definition of torsion angles. [b] Reference 4, there are four crystallographically independent molecules. [c] Reference 5, there are three crystallographically independent molecules. [d] Reference 6, coordinates from NMR and model building.

(44) Cervantes-Lee, F.; Porter, L. C. *Acta Crystallogr.* **1991**, *C47*, 2312−2315.

Table 4. Phosphate Backbone and 4-aminoTEMPO Torsion Angles for *cis*-Diamineplatinum(II) d(GpG) Complexes Derived from X-ray Crystal Structures and Molecular Mechanics Minimization with and without NMR Constraints[a]

	phosphate backbone				4-aminoTEMPO	
structure	ϵ	ζ	α	β	Pt−N	N−C
J+NO d(GpG)	−133	−67	−64	174	150	−74
J d(GpG)	−141	−14	−167	−144	−162	−123
NO d(GpG)	−132	−50	−84	−150	−161	−172
MM d(GpG)	−122	−84	53	119	152	−103
d(pGpG) 1[b]	−142(3)	−65(3)	−85(8)	−143(6)		
d(pGpG) 2[b]	−144(3)	−64(3)	−77(6)	−141(4)		
d(pGpG) 3[b]	−126(4)	−71(5)	−57(7)	−168(6)		
d(pGpG) 4[b]	−128(4)	−69(4)	−49(5)	−161(4)		
d(CpGpG) 1[c]	−148(4)	−50(5)	−112(7)	163(5)		
d(CpGpG) 2[c]	−132(4)	−64(4)	−60(6)	187(4)		
d(CpGpG) 3[c]	−152(5)	−67(6)	145(10)	164(6)		
d(GpG)[d]	−157	−53	−68	−168		

[a] See Chart 2 for definition of torsion angles. [b] Reference 4, there are four crystallographically independent molecules. [c] Reference 5, there are three crystallographically independent molecules. [d] Reference 6, coordinates from NMR and model building.

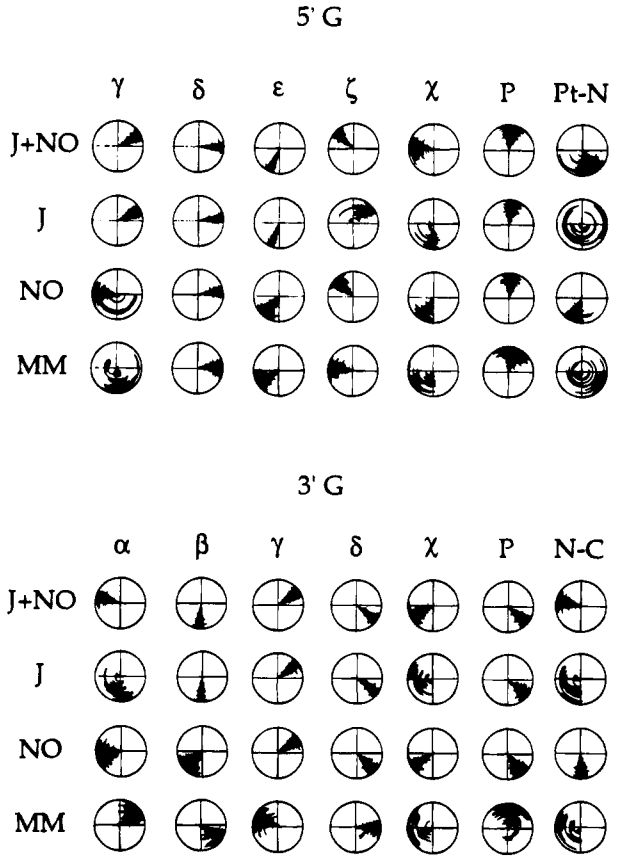

Figure 6. Conformational dials analysis of torsion angles (Chart 2) during dynamics trajectory for the 5′ orientational isomer of *cis*-[Pt(NH$_3$)(4-aminoTEMPO){d(GpG)}]$^+$ (**13**). The radial coordinate is time and it varies from 0 ps at the center to 200 ps at the circumference. The top of the circle is 0° and the angle increases clockwise to 360°.

unconstrained dynamics (MM) agree with the experimental data from X-ray and NMR (Figure 6). These torsion angles are apparently constrained by the 17-membered Pt-d(GpG) chelate ring formed by coordination of the two adjacent purine base N(7) atoms. The ability of the force field to constrain ϵ to the correct (ϵ^-) conformation indicates that it was not necessary to use the *J*-coupling constant between 3′-H$_{3'}$ and ^{31}P, derived from the *cis*-[Pt(NH$_3$)$_2${d(GpG)}]$^+$ NMR structure determination.[6] Although inclusion of the *J*-coupling constraint reduced the motion of the ϵ torsion angle in dynamics calculations, it did not significantly alter ϵ from its value in the unconstrained dynamics (MM) (Figure 6).

Addition of paramagnetic nitroxide-to-^{1}H and ^{31}P distance constraints (NO) to the refinement of **13** allowed the force field accurately to mimic the torsion angle ranges observed for X-ray and NMR determinations of d(GpG) bound to cisplatin, except for the 5′-γ and χ torsion angles.[4-6] The difficulty in fixing the 5′-γ torsion angle may have been due to a combination of the close distance between the 5′ methylene protons and the unpaired electron and unhindered rotation about the 5′-γ torsion angle. As the line width for protons close to the unpaired electron increased (50−100 Hz), so did the error in determining the paramagnetic relaxation time (Tables 1 and S2).

Structure refinements that included torsional information from coupling constants (*J*) for the diamagnetic complex constrained the force field to torsion angles consistent with X-ray and NMR structures of cisplatin-modified d(GpG), except for the ζ and α torsion angles in the phosphodiester backbone (Chart 2). *J*-coupling and nOe NMR data are not available to constrain the ζ or α torsion angles in oligonucleotides.[7] Both the ^{31}P NMR chemical shift and the absence of H$_{1'}$ to H$_{5'}$/H$_{5''}$ proton nOe's have been used to constrain indirectly the ζ or α torsion angles. In the assignment of the *cis*-[Pt(NH$_3$)$_2${d(GpG)}]$^+$ solution structure, the ^{31}P NMR chemical shift was used to determine that ζ and α were both in a gauche form, and the ζ^- and α^- gauche forms were chosen because they had the least offensive van der Waals interactions in model building.[6] The dynamics trajectories for **13** clearly revealed that use of only backbone dihedral constraints (*J*-coupling) allowed ζ and α torsion angles to sample both ζ^-, α^- and ζ^+, α^t conformational space (Figure 6).

Figure 6 also shows the affects of combining paramagnetic distances and *J*-coupling constants (J+NO) into the constrained dynamics of **13**. A sum of *J*-coupling and nitroxide-to-^{1}H and -^{31}P distances resulted in conformers for **13** that agreed with all of the crystallographic and NMR determined torsion angles for known cisplatin-modified d(GpG)-containing complexes. A distinct advantage of combining paramagnetic NMR constraints was observed in the determination of ζ and α torsion angles of the phosphodiester backbone. The incorporation of both dihedral and paramagnetic constraints (J+NO), or only the paramagnetic constraints (NO), into the dynamics trajectories for **13** limited the phosphodiester backbone to sample only the ζ^-, α^- conformation observed by X-ray crystallography and proposed by NMR spectroscopy and model building.[4-6] These distances to the PO$_4$ moiety and backbone protons in **13**, determined with the aid of the paramagnetic spin probe, provide the first observable NMR constraints for determining the configuration of the ζ or α torsion angles in oligonucleotides.[7,45,46]

The optimal χ torsion angles for the *cis*-[Pt(NH$_3$)$_2${d(GpG)}]$^+$ solution structure were also obtained from model building, since no ^{1}H NMR constraints were available to determine them. The dynamics trajectories (Figure 6) demonstrated the χ torsion angles for both the 5′ and 3′ guanosine rings of **13** to be more highly constrained by the addition of paramagnetic NMR constraints. χ could be even more accurately determined by obtaining paramagnetic constraints for the exchangable protons of the guanosine rings from ^{1}H NMR relaxation measurements in H$_2$O solutions, or by incorporating ^{13}C and ^{15}N labels at specific sites in the dinucleotide.

(45) Kim, S. G.; Lin, L. J.; Reid, B. R. *Biochemistry* **1992**, *31*, 3564−3574.
(46) Robinson, H.; Wang, A. H. J. *Biochemistry* **1992**, *31*, 3524−3533.

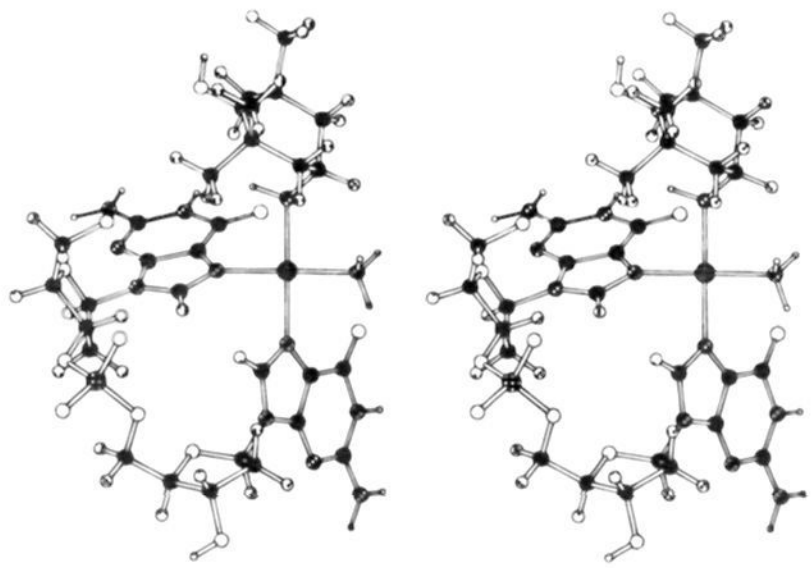

Figure 7. Stereo view of the structure obtained following dynamics averaging and minimization of the 5′ orientational isomer of *cis*-[Pt(NH$_3$)(4-aminoTEMPO){d(GpG)}]$^+$ (**13**) applying both diamagnetic and paramagnetic (J+NO) constraints.

Motion of the 4-aminoTEMPO ligand with respect to the d(GpG) ligand was observed by changes in the Pt−N$_{TEMPO}$ and N$_{TEMPO}$−C$_{TEMPO}$ torsion angles (Figure 6). NMR-derived nOe data cannot be obtained between protons separated by more than 5 Å, but the introduction of paramagnetic constraints can correlate the motion of two functional groups over a distance of 12−15 Å.[13,14,16] Inspection of the 300 K dynamic trajectories revealed important differences in conformational space available to the 4-aminoTEMPO ligand. The unconstrained (MM) and dihedral constrained (*J*) dynamics trajectories showed free rotation about the Pt−N$_{TEMPO}$ bond, but trajectories constrained by only paramagnetic (NO) and combined dihedral and paramagnetic constraints (J+NO) remained in a single conformational family. The difference between trajectories constrained by paramagnetic (NO) and combined paramagnetic and *J*-coupling constraints (J+NO) was due to the change in 5′-γ torsion angle from γ^+ to γ^t in the paramagnetic (NO) constrained trajectory. When the 5′-γ torsion was in the γ^t conformation, the methylene protons were in close van der Waals contact with the 4-aminoTEMPO ligand, leading to a different dihedral angle about the Pt−N$_{TEMPO}$ bond. Dynamics trajectories with combined paramagnetic and *J*-coupling constraints (J+NO) were also obtained with Pt−N$_{TEMPO}$ and N$_{TEMPO}$−C$_{TEMPO}$ torsion angles in randomized starting orientations. After 200 ps of dynamics at 300 K, the Pt−N$_{TEMPO}$ and N$_{TEMPO}$−C$_{TEMPO}$ torsion angles always returned to the conformational families shown in Figure 6. The observation of two sets of methyl resonances in the ^{1}H NMR spectrum for **13** revealed the 4-aminoTEMPO ligand to undergo motional averaging on the NMR time scale. Thus, the 4-aminoTEMPO ligand in **13** is not as rigid on the NMR time scale as in longer oligonucleotides (vide infra). Although we cannot define this motion from our computational analysis, the dynamics trajectories favor a hindered rotational model, which averages the magnetic environment observed by the methyl groups. The motional averaging does not limit the accuracy of our structure determination, as discussed below.

A stereo view of the averaged structure for **13**, displaying the combined effects of paramagnetic and diamagnetic constraints (J+NO), is shown in Figure 7. All twelve of the dihedral constraints were satisfied and four of the paramagnetic (NO) constraints were satisfied. Seven of the paramagnetic constraints were longer than calculated upper bounds (total violation of 1.25 Å), and the largest deviation was the distance to the 3′-H$_{5''}$ proton (0.51 Å). Five of the paramagnetic distances were shorter than calculated lower bounds (total violation of 1.17 Å), the greatest deviation belonging to the 3′-H$_{3'}$ proton (0.32 Å). The large deviation of these protons from the paramagnetic distance boundaries could be related to their position in the 1-D ^{1}H NMR spectrum. Overlap of the 3′-H$_{5''}$ and 3′-H$_{5'}$ protons and the overlap of the 3′-H$_{3'}$ proton with the HDO resonance could affect the interpretation of the 1-D T_1 and T_2 relaxation time measurements. Obtaining T$_1$ and T$_2$ relaxation times from 2-D NMR spectra would increase the spectral dispersion for these and other resonances to allow for determining unique relaxation times of protons overlapped in the 1-D NMR spectrum. Dynamics trajectories with increased upper and lower bounds for protons overlapped in the 1-D spectrum did not lead to results significantly different from those for the original constrained dynamics calculation (RMSD all non-hydrogen atoms 0.40 Å), and only afforded fewer violations of upper and lower bound constraints.

The behavior of the 5′-ν_{max} and 3′-ν_{max} torsion angles during dynamics (Figure S2) demonstrated that the force field parameters and constraints restricted the motion to ±15°, and these values were only slightly perturbed by the addition of diamagnetic or paramagnetic NMR constraints. The Pt-α torsions were constrained by parameters from a previous molecular mechanics study.[10] The Pt−N(7) vector remained within ±18° of the normal to the plane of the guanosine ring, in agreement with X-ray crystallographic data.[4,5] Two preferred orientations for the Pt-β torsion angles, designated L$_1$ and R$_2$, have been described for *cis*-{Pt(NH$_3$)$_2$}$^{2+}$ d(GpG) adducts in oligonucleotides.[39] The L$_1$ conformation has its 5′ Pt-β torsion angle between −90° and −160°, whereas the 3′ Pt-β torsion angle lies between 30° and 160°. For the R$_2$ conformation, the 5′ Pt-β torsion angle lies between −30° and −160°, and the 3′ Pt-β torsion angle lies between 90° and 160°. The Pt-β torsion angles were not constrained by explicit torsional barriers in our force field, and they sample a variety of ranges dependent upon the constraints used in the dynamics. In the MM calculation, the Pt-β torsion angles indicated that at the beginning of the dynamics trajectory the complex was in an L$_1$ conformation, but it finished in the R$_2$ conformation. The *J*-constrained trajectory sampled both the L$_1$ and R$_2$ conformations during 200 ps of dynamics, but with a smaller range of motion than the unconstrained MM trajectory. The NO and J+NO constrained refinements maintained two slightly different R$_2$ conformations for the entire dynamics trajectory, which was in agreement with the 5′ H$_8$ ^{1}H NMR chemical shift being downfield of the 3′ H$_8$ resonance for **13** in dilute (1 mM) solution. Additional paramagnetic NMR constraints to exchangeable base protons or to specific ^{13}C and ^{15}N labels would allow for a more accurate determination of Pt-β torsion angles.

Errors in the paramagnetic constraints determined here could be introduced by motional averaging of the 4-aminoTEMPO ligand or the d(GpG) chelate ring. Either motion can be addressed by defining a population of states, the paramagnetic contributions from which will sum to the overall measured relaxation rate. For nucleotides, a simple two-state model of S (C2′-endo) and N (C3′-endo) conformers has been used to explain the observed *J*-coupling constants within the deoxyribose ring. An analogous description can be used to understand the affects of motional averaging to paramagnetic relaxation, as shown for two conformations in eq 6. The total relaxation rate,

$$\frac{1}{T_{1\text{para total}}} = \chi_A \frac{1}{T_{1\text{para A}}} + \chi_B \frac{1}{T_{1\text{para B}}} \qquad (6)$$

($T_{1\text{para total}}$)$^{-1}$, will be a sum of the individual rates for states A and B times the mole fraction (χ) for each state. For cisplatin-modified d(GpG), the conformation of the 3′ deoxyribose ring was assigned as approximately 70% S from ^{1}H NMR *J*-coupling

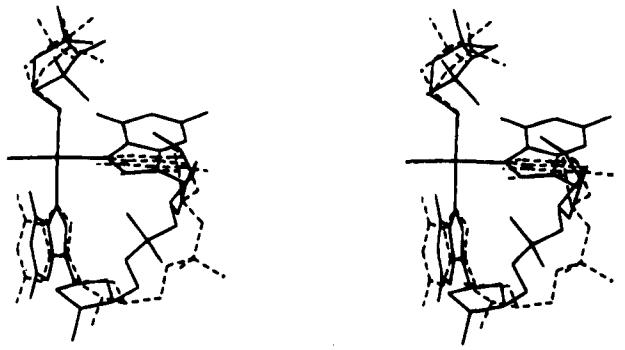

Figure 8. Stereo view of structures obtained following dynamics averaging and minimization with *J*-coupling (J, dashed line), or a sum of dihedral constraints and paramagnetic distances (J+NO, solid line), of the 5′ orientational isomer of *cis*-[Pt(NH$_3$)(4-aminoTEMPO)-{d(GpG)}]$^+$ (**13**) in which the platinum and coordinated nitrogen atoms have been superimposed.

constants. Starting from the coordinates for **13** determined from a combination of diamagnetic and paramagnetic constraints (J+NO), we varied the conformation of the 3′-deoxyribose ring from 100% S or 100% N and determined the paramagnetic distances for all of the protons within the deoxyribose ring. The largest change in nitroxide-to-proton distance occurred for the H3′ proton (1.5 Å), readily distinguishing the two conformational models. The observed relaxation rates for the 3′-deoxyribose ring predicted a 70−80% S population, in agreement with the diamagnetic *J*-coupling constant data. This agreement strongly validates the use of averaged unpaired electron spin density of the 4-aminoTEMPO ligand in the structure determination of **13**.

Figure 8 presents a stereo view of the average diamagnetic (J, dashed line) and combined paramagnetic and diamagnetic (J+NO, solid line) structures in which the Pt and coordinating nitrogen atoms have been superimposed. The deoxyribose phosphodiester backbones of the two structures obtained from the constrained dynamics trajectories share little similarity, illustrating the importance of including paramagnetic distance information in the refinement of the solution structure of **13**.

Summary and Conclusions

The synthesis of paramagnetic Pt(II) complexes has allowed for the determination of several important structural properties of DNA containing the 1,2-intrastrand *cis*-diamineplatinum(II) d(GpG) cross-link. The selective broadening of ^{1}H NMR resonances adjacent to the 4-aminoTEMPO ligand facilitated the assignment of the asymmetric 3′ (**12**) and 5′ (**13**) orientational isomers of *cis*-[Pt(NH$_3$)(4-aminoTEMPO){d(GpG)}]$^+$ from simple inspection of line widths in 1-D ^{1}H NMR spectra. From relaxation measurements (T_{1para}) in 1-D NMR spectra we could determine accurate 6−12 (±0.5) Å long-range distance constraints for use in the computational refinement of cisplatin-modified nucleotides. The complementary addition of dihedral (*J*-coupling) and paramagnetic nitroxide-to-proton and nitroxide-to-phosphorus distance constraints to computational methods resulted in a conformation of *cis*-[Pt(NH$_3$)(4-aminoTEMPO)-{d(GpG)}]$^+$ (**13**) (Figure 6) that was highly constrained during dynamics trajectories, and accurate when compared with NMR and X-ray crystallographic structures of d(GpG) complexes modified by cisplatin.[4-6] The addition of paramagnetic NMR constraints allowed the determination of ζ and α phosphodiester torsion angles for which no diamagnetic NMR data are available. The extension of this paramagnetic constraint methodology to duplex DNAs modified by the cisplatin paramagnetic analogue *cis*-[Pt(NH$_3$)(4-aminoTEMPO)Cll] (**7**) is in progress.

Acknowledgment. This work was supported by Grant No. CA 32134 from the National Cancer Institute. S.U.D. is grateful to the National Institutes of Health for a Postdoctoral Research Fellowship. We thank C. Luchinat (Bologna) and I. Bertini (Florence) for valuable discussions and L. Chassot (Ciba-Geigy, Research Center Marly) and M. Karplus (Harvard) for assistance with CHARMm parameter optimization.

Supporting Information Available: Tables of resonance assignments, T_{1para} and T_{2para} relaxation parameters, and $\tau_{c\ e\text{-}n}$ for **7**, **12**, and **13**, ^{1}H NMR chemical shift versus pH titration for **12** and **13**, and conformational dials analysis for 5′ and 3′ Pt-α, Pt-β, and ν_{max} torsions of **13** (6 pages). This material is contained in libraries on microfiche, immediately follows this article in the microfilm version of the journal, can be ordered from the ACS, and can be downloaded from the Internet; see any current masthead page for ordering information and Internet access instructions.

JA950839S

(47) **Note Added in Proof**: Since this article was submitted we solved the X-ray structure of a cisplatin-modified DNA duplex dodecamer to 2.6 Å resolution (Takahara, P. M.; Rosenzweig, A. C.; Frederick, C. A.; Lippard, S. J. *Nature* In press).